

SHEET FAILURE PREDICTION DURING FORMING OF ADVANCED HIGH STRENGTH STEELS

D. Gutiérrez^{1*}, R. Hernández^{1,2}, A. Lara¹, D. Casellas^{1,2}, M.D. Riera^{1,2}, J.M. Prado^{1,3}

¹Fundació CTM Centre Tecnològic, Av. Bases de Manresa, 1, 08242 Manresa, Spain.

david.gutierrez@ctm.com.es; ricardo.hernandez@ctm.com.es;

toni.lara@ctm.com.es; daniel.casellas@ctm.com.es; md.riera@ctm.com.es

²Department of Materials Science and Engineering Metallurgy Universitat Politècnica de Catalunya, EPSEM, Av. Bases de Manresa 61, 08242 Manresa, Spain.

³Department of Materials Science and Engineering Metallurgy Universitat Politècnica de Catalunya, Av. Diagonal 647, 08028 Barcelona, Spain.

jm.prado@ctm.com.es

ABSTRACT: The automotive industry has increased significantly the use of advanced high strength steels (AHSS) in many structural components of vehicles, with the aim to reduce weight and also increase safety. The high resistance of these steels is accompanied by a decrease in formability, which makes simulation a requirement to adequately foresee the formability of a stretch formed component. For sheet metal forming, the conventional diagram based in strains, Forming Limit Diagrams (FLD), is often used as a failure criterion, but this approach is not effective when working with AHSS, due to the bigger effect produced by changes on strain paths than conventional steels. This work proposes the use a Forming Limit Stress Diagram (FLSD) based on the main stresses acting on the material. These FLSD has been obtained by the simulation of stretching test. To improve the results, the tensile test curve has been extended by using an optical measuring system and a subsequent adjustment of the stress-strain curve for the material. Finally, simulations and real parts behavior have been compared and the failure predictions models have been discussed.

KEYWORDS: FLC, FLSC, formability, optical measuring system, AHSS.

1 INTRODUCTION

The automotive industry pays great attention to development of new steel grades that combine high strength and good formability. Stimulated for these needs in the transport area, the steelmakers have been developed the advanced high strength steels (AHSS) that have allowed reducing thickness in body parts.

On the other hand, the formability in sheet metals has widely been described by the Forming Limit Diagrams (FLDs) and their Forming Limit Curve (FLC). But these curves are highly path dependent, which makes this method rather ineffective to analyze complex forming processes. In addition, this effect is greater in the current AHSS [1, 2], because depending on the stretching test used to obtain FLC (Nakajima or Marciniak tests), different FLCs are achieved. The analysis based on the Forming Limit Stress Diagrams (FLSDs) and the associated limit stress curve (FLSC) has received major attention in recent years, because

the FLSC is less sensitive to the strain path effect than the FLC [3].

Moreover, AHSS may fail without necking, through premature ductile fracture. Accordingly, many researchers consider two different failure criterion, the necking failure criterion, FLC, and fracture failure criterion, FLCF (Forming Limit Curve at Fracture) [4]. In the same way, it can be defined two failure criterion for FLSC; the FLSC as necking failure criterion and FLSCF (Forming Limit Stress Curve at Fracture) as fracture failure criterion.

The experimental evaluation of FLSC or FLSCF needs the transformation of strain space to tension space according to Lévy-Mises flow law [5]. But another option is using Finite Element Method (FEM) in the simulations of stretching test as Nakajima or Marciniak [6].

The proper simulation of the stretching tests requires knowing the hardening law that

* Corresponding author: postal address, phone, fax, email address

characterize the material. Uniaxial tensile test is the common method to obtain the mechanical properties in sheet metals. This test is quite useful when the range of deformations that a workpiece will undergo is not very large. However the test is not appropriate when the material is formed in multiaxial directions, where the material suffers more deformation before necking or fracture. This problem can be solved using other tests to provide greater deformation before the necking or the fracture event.

In this sense, the compression test allows to develop larger deformation. Metals in this type of tests generally withstand greater deformation, making it very useful to extend the stress-strain curve of the material. The compression test is performed by axially pressing a solid cylinder specimen. In sheet metals, the stack compression test proposed by Pawelski [7] in 1967 is used to evaluate the flow curve. The test makes use of circular discs that are cut out of the blanks and stacked to form a cylindrical specimen with an aspect ratio in the range of solid cylinders currently employed in the conventional compression test [8, 9, 10].

Other methods to extend the flow curve involve calculating the deformation when necking occurs in the uniaxial tensile test. In this case, by optical measuring systems is possible to determine the strains during the entire test [11], allowing to calculate the deformation during the necking phenomenon.

Therefore, the objective of this work is to determine the FLSC and FLSCF in AHSS from FLC and FLCF obtained by the Nakajima and Marciniak stretching test using FEM. To determine the stress states, it has been used an extension of stress-strain curves by stack compression test and uniaxial tensile test using an optical measuring system. Finally, computer simulations and real parts behavior have been compared and the failure predictions models have been discussed.

2 MATERIALS

Two grades of AHSS were tested, two Dual-Phase steels: DP780 and DP1000 with thicknesses of 1.5mm and a TRIP steel: TRIP800 with a thickness of 2.0mm.

Table 1 shows the chemical composition of the tested steels. The microstructures were revealed by etching with Nital 2%, Fig. 1 and 2. The Dual Phase steels show martensitic matrix with ferrite in grain boundaries. Meanwhile, the microstructure of TRIP800 steel show the martensite/bainite (dark phases) and ferrite/retained austenite (grey phases).

Table 1: Chemical composition.

Material	%C	%Si	%Mn	%Cr	%Ni	%Al	%Nb
TRIP800	0.20	1.61	1.73	0.02	0.03	0.04	0.01
DP780	0.13	0.21	1.89	0.18	0.04	0.03	0.01
DP1000	0.18	0.21	1.83	0.51	0.04	0.05	0.01

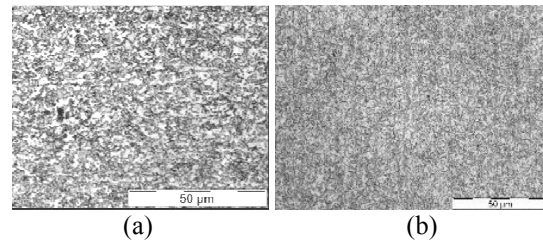


Fig. 1 Microstructure of Dual Phase steels. a) DP780 steel and b) DP1000 steel.

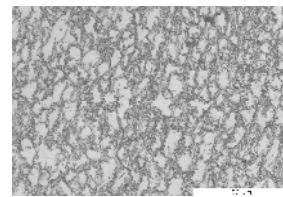


Fig. 2 Microstructure of TRIP800 steel.

3 EXPERIMENTAL PROCEDURE

3.1 MECHANICAL CHARACTERIZATION

Tensile and compression tests are performed in an INSTRON 250kN universal testing machine.

3.1.1 Stack compression test

A conventional testing method as tensile test is not applicable for the compression test because of buckling of a specimen. So, in order to apply a compressive load to the metal sheets, it must be available a set of stacked discs, which are arranged in a tool to obtain a correct alignment between the discs, Fig. 3a. The resulting specimen should not exceed a buckling limit of 1.5 (ratio of height to diameter cylinder). To avoid frictional effects between the faces of the specimen and the compression plates, the test pieces are wrapped with Teflon, as shown in Fig 3b.

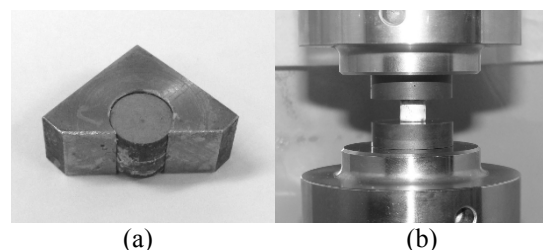


Fig. 3 a) Stack compression test specimen). b) Stack compression test specimen wrapped with Teflon before test.

3.1.2 Optical measuring system

In an uniaxial tensile test strain is measured using conventional extensometer or videoextensometer. The measurements are carried out between two points in a calibrated area, so it is not possible to accurately measure the strain during localized necking. Nowadays, with optical strain measuring systems it is possible to follow the strain during the entire test, even in necking stage. In this work, the strains were calculated by ARAMIS software, a system for optical 3D deformation analysis developed by GOM mbH. This software is based on two CCD cameras, which observe the deformation surface. A stochastic pattern must be applied (by spray painting) on the sample surface to allow following the deformation, Fig. 4 [11].

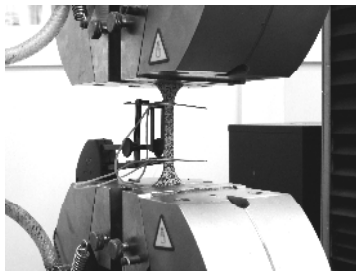


Fig. 4 Testing device in tensile test. Specimen with stochastic pattern (ARAMIS) and extensometer.

3.2 FLC & FLCF

The FLCs have been acquired according by stretching tests to the procedure described in references [1] and [2]. The necking was calculated according to mathematical method proposed in ISO12004 standard [12]. The strains in FLCF are obtained in the stage before fracture, according to maximum deformations obtained by ARAMIS software.

3.3 FORMING PROCESS

In order to validate the strain and stress failure criterion a specific workpiece was designed, with an important change in section aimed at producing a nonlinear deformation path. The forming process were carried out in a hydraulic press. The tool has a bottom and top press-holders and a punch to provide the form to the sheet. Fig. 5 shows the tool to produce the forming and the specimen after the deformation.

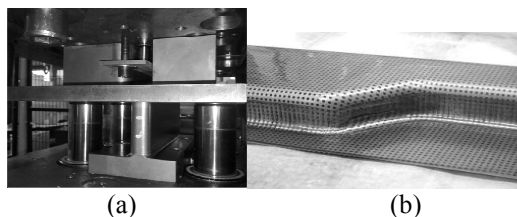


Fig. 5 a) Tool to produce the forming. b) Specimen obtained after the deformation.

3.4 NUMERICAL SIMULATION

The simulation of Nakajima and Marciniak stretching tests and the forming process were carried out with ABAQUS/Explicit. According to symmetrical boundary conditions in stretching tests, only one quarter of the model is simulated. The analysis is carried out with shell linear elements S4R.

Fig. 6 shows some examples about the models used in ABAQUS simulations.

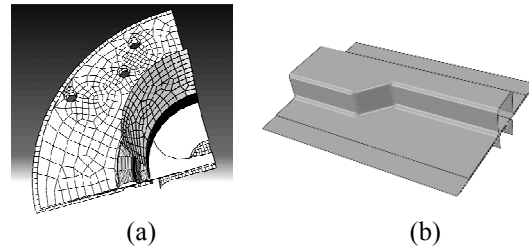


Fig. 6 a) Marciniak and b) forming models in ABAQUS/Explicit simulations.

4 RESULTS AND DISCUSSION

4.1 FLOW CURVES

Fig. 7 shows the flow curves in DP780 steel obtained by tensile and stack compression tests. The flow curve calculated according to ARAMIS method provide good agreement with experimental data obtained with extensometer. Meanwhile the flow curve acquired by stack compression test provides less concordance with data obtained with the extensometer.

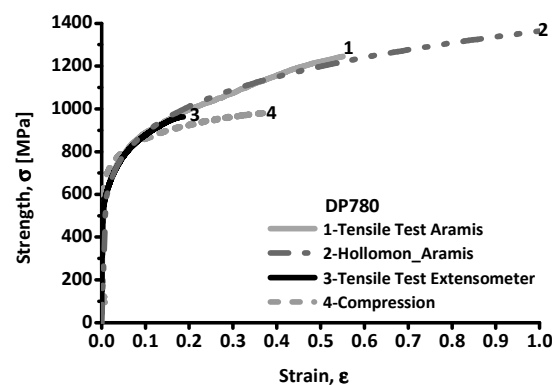


Fig. 7 Flow curves in DP780 steel.

Fig. 8 shows the flow curves in DP1000 steel obtained by tensile and stack compression tests. The flow curves have the same trend as DP780 steel, a better agreement with ARAMIS method.

Fig. 9 shows the flow curves in TRIP800 steel obtained by tensile and stack compression tests. The flow curves obtained by stack compression test provides less concordance and a large strains the tension decrease, because buckling phenomenon

could be produced. On the other hand, ARAMIS method presents a great agreement with extensometer results.

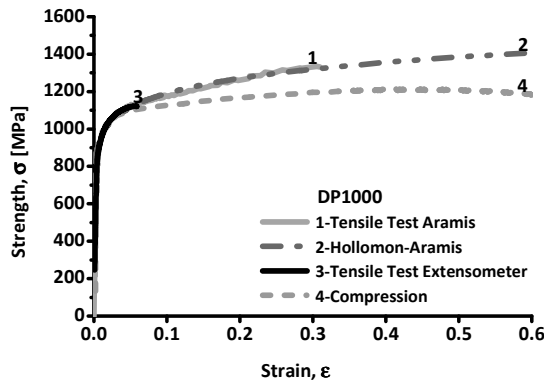


Fig. 8 Flow curves in DP1000 steel.

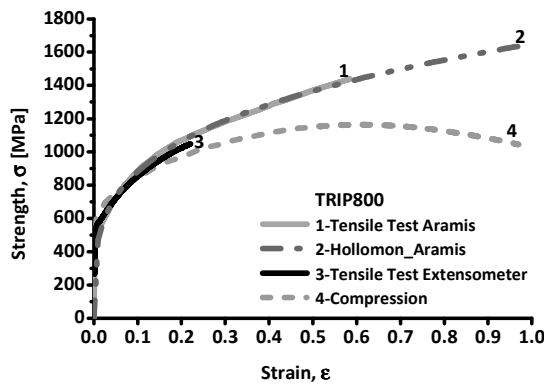


Fig. 9 Flow curves in TRIP800 steel.

As shown in Fig. 7-9 ARAMIS method provides an excellent tool to obtain a larger flow curves in AHSS. In the tested materials, a hardening law as Hollomon can be fitted in ARAMIS flow curve:

$$\sigma = k\epsilon^n \quad (1)$$

4.2 FORMING LIMIT STRESS CURVES

To obtain the FLSC it is required to have the FLC and the flow curves. They were obtained by fitting the results to a Hollomon hardening law using ARAMIS method as seen above.

The simulation of stretching tests has been validated with experimental results according to the strain path obtained from different samples. So, Fig. 10 and 11 show the strain paths obtained in experimental test (with optical strain measurement, ARAMIS) and simulation (ABAQUS) in TRIP800 steel. As shown in these figures, there is a good correlation in the strain paths, between experimental and simulation results.

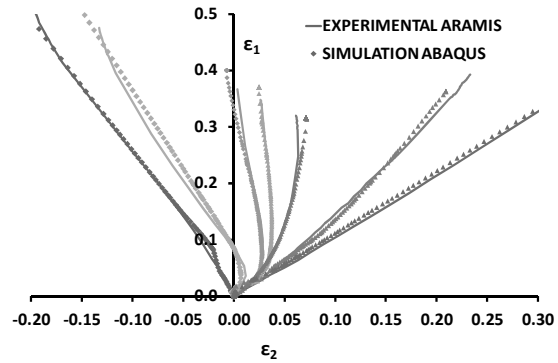


Fig. 10 Strain path obtained by experimental and simulation from Nakajima test in TRIP800 steel.

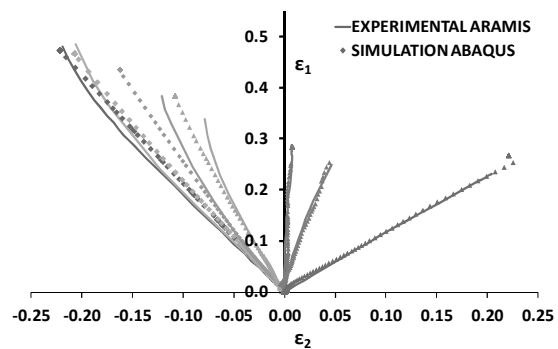


Fig. 11 Strain path obtained by experimental and simulation from Marciniak test in TRIP800 steel.

Fig. 12 and Fig. 13 show the FLSC and FLSCF obtained by Nakajima and Marciniak stretching tests in TRIP800 steel.

The FLSC and FLSCF have some differences depending on the stretching test used. The Nakajima test typically shows non-linear strain paths, which provide more deformation in some areas of FLD. It implies that FLSC and FLSCF in TRIP800 steel are also different as the FLC and FLCF obtained by Nakajima and Marciniak tests.

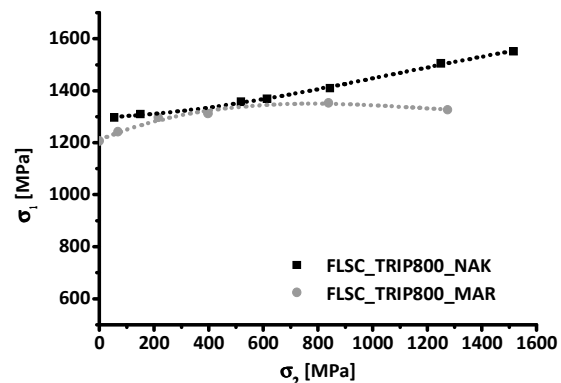


Fig. 12 FLSC in TRIP800 steel.

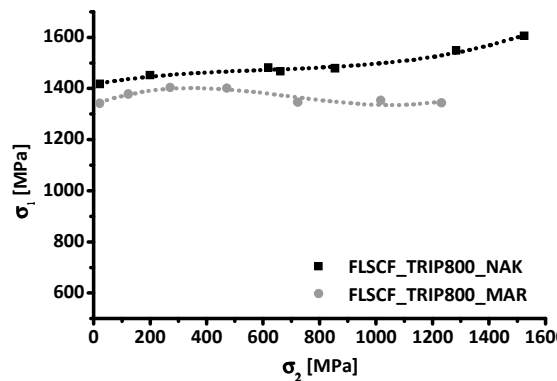


Fig. 13 FLSCFs in TRIP800 steel.

Fig. 14 shows the FLC and FLCF in TRIP800 steel, where some differences in position and deformation between Nakajima and Marciniak stretching tests can be discerned.

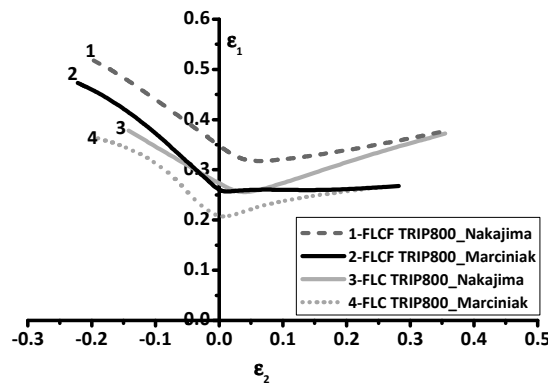


Fig. 14 FLCs and FLCFs in TRIP800 steel.

According to literature [3, 5] FLSC curves are independent or less sensitive of the strain paths, but the stress forming limit are obtained of FLC which are strain path dependent, so FLSC would be also influenced by the changes in the strain paths. This dependence should be greater or lesser depending on the hardening law. Some authors have shown different FLSC according to using a hardening law as Hollomon or Voce [13]. The resulting FLSCF, using a Voce hardening law, is pictured in Fig. 15.

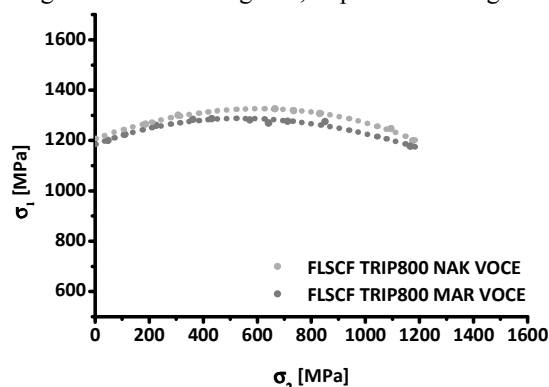


Fig. 15 FLSCFs in TRIP800 steel with Voce hardening law.

It can be seen that there are less differences between the FLSCF obtained by the Nakajima and Marciniak stretching test. In this case, the FLSCF obtained by Voce hardening law is less sensitive to changes in strain paths.

4.3 FAILURE PREDICTIONS IN FORMING SIMULATIONS

In order to validate the strain and stress failure criterion, the FEM results and the experimental ones were compared. The drawing depth obtained until necking and fracture was 27 and 31mm, respectively. Fig. 16 shows the drawing depth obtained with FEM by the different necking failure criterion and the experimental results for TRIP800 steel. Fig. 17 shows similar results in the fracture failure criterion.

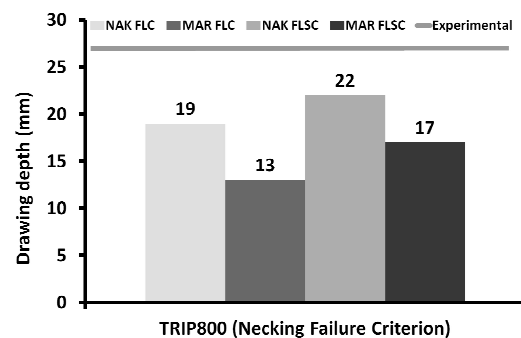


Fig. 16 Necking failure criterion in TRIP800 steel.

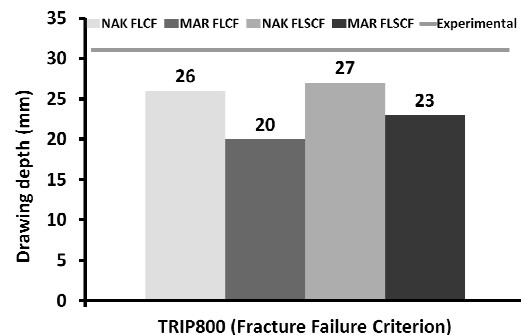


Fig. 17 Fracture failure criterion in TRIP800 steel.

The results in TRIP800 steel show that Nakajima test provides better results than Marciniak test. Also, the failure criterion according to stresses presents a good agreement with experimental results. These results are according to previous works in AHSS [10], but in this case the authors do not differentiate between necking and failure criterion.

However, the prediction obtained by the strains fracture failure criterion is very similar to those obtained with the stress fracture criterion. This remark is also seen in DP780 steel, where the experimental drawing depth at fracture was 23mm.

Fig. 18 shows the fracture failure criterion, where FLSCF provides a better result than FLCF, but there is no important differences than in necking failure criterion [10].

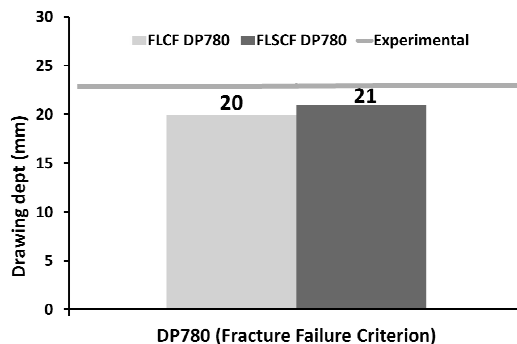


Fig. 18 Fracture failure criterion in DP780 steel.

5 CONCLUSIONS

Based on the experimental results of the flow curves, forming process and the FEM, the following conclusions can be drawn from the present work:

The flow curve calculated according to ARAMIS method is a good alternative to other tests as compression or hydraulic bulge test.

In TRIP800 steel, the FLSCs have some differences depending on the stretching tests; these variations are similar in the FLCs. The applied hardening law has a marked influence when to calculating the corresponding FLSCs.

In general, the failure criterion based on stress provides better results than the one based on strains. The FLCF is a good failure prediction in fracture criteria.

6 ACKNOWLEDGEMENT

This work was partially funded by ACC10 (TECCTA11-1-0006).

REFERENCES

- [1] Gutiérrez D., Lara A., Casellas D., Prado J.M.: *Effect of strain paths on formability evaluation of TRIP steels*. Advanced Materials Research 89-91, 214-219, 2010.
- [2] Gutiérrez D., Lara A., Casellas D., Prado J.M.: *Strain paths effects on the formability of advanced strength steels evaluated by stretching tests*. In: Proceedings of the 49 th IDDRG 2009 International Congress, 491-502, 2009.
- [3] Stoughton T.: *A general forming limit criterion for sheet metal forming*. International Journal of Mechanical Sciences. Vol. 42, 1-27, 2000.
- [4] Tasan C.C., Hoefnagels J.P.M., ten Horn C.H.L.J., Geers M.G.D.: *Experimental analysis of strain path dependent ductile damage mechanics and forming limits*. Mechanics of Materials 41, 1264-1276, 2009.
- [5] Arrieux R., Bedrin C., Boivin M.: *Determination of an intrinsic forming limit stress diagram for isotropic metal sheets*. In: Proceedings of the 12th IDDRG International Congress, 61-71, 1982.
- [6] Uthaisangsuk V., Prah U., Bleck W.: *Stress based failure criterion for formability characterization of metastable steels*. Computational Materials Science 39, 43-48, 2007.
- [7] Pawelski O.: *Über das Stauchen von Holzyindern und seine Eignung zur Bestimmung der Formänderungsfestigkeit dünner Bleche*. Archiv für Eisenhüttenwesen 38, 437-442, 1967.
- [8] Alves L.M., Nielsen C.V., Martins P.A.F.: *Revisiting the Fundamentals and Capabilities of the Stack Compression Test*. Experimental Mechanics 51, 1565-1572, 2011.
- [9] Merklein M., Kuppert A.: *A method for the layer compression test considering the anisotropic material behaviour*. Int J Mater Form 12, 483-486, 2009.
- [10] Hernández R., Llobet A., Gomez X., Riera M.D.: *FLSD as a good choice in sheet forming of AHSS*. SIMULIA Customer Conference 2011.
- [11] Gutiérrez D., Lara A., Casellas D., Prado J.M.: In: *Application of optical strain measuring systems to determine plastic anisotropy and theoretical forming limit curves in AHSS*. Proceedings of the 50th IDDRG 2010 International Congress (ISBN 978-3-85125-108-1), 2010.
- [12] ISO standard 12004. *Metallic materials – Guidelines for the determination of FLD*. 2008.
- [13] M.C. Butuc. *Forming Limit Diagrams. Definition of plastic instability criteria*. PhD. FEUP, University of Porto, 2004.